RSC Advances

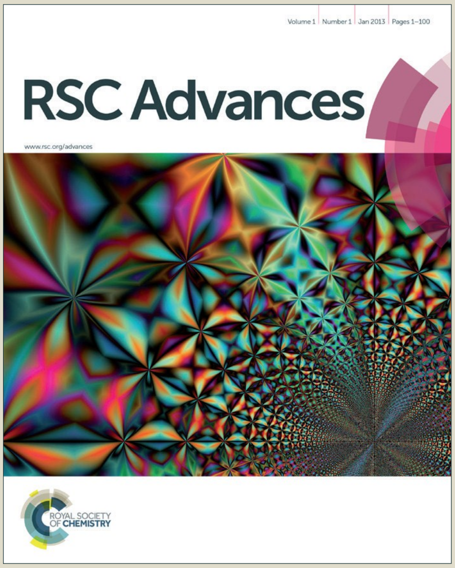

ROYAL SOCIETY OF CHEMISTRY

www.rsc.org/advances

Poling Efficiency (r_{33}/N)

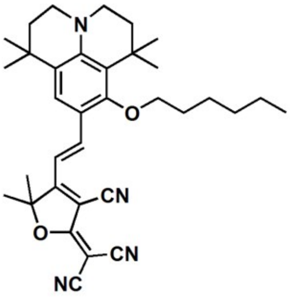

C1

8.971×10^{-20} pm g/(V molecules)

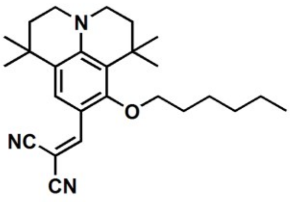

C2

1.01×10^{-20} pm g/(V molecules)

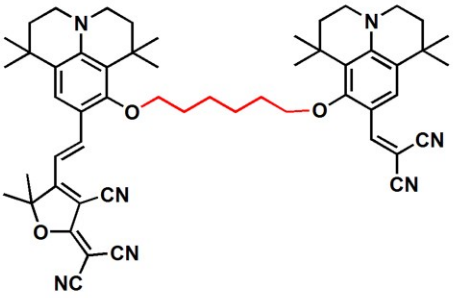

C3

10.71×10^{-20} pm g/(V molecules)

Journal Name RSCPublishing

ARTICLE

Cite this: DOI: 10.1039/x0xx00000x

Received 00th January 2012,
Accepted 00th January 2012

DOI: 10.1039/x0xx00000x

www.rsc.org/

Improving poling efficiency by synthesizing of a nonlinear optical chromophore containing two asymmetric non-conjugated D-π-A chains†

Shengyu Cong,[ab] Airui Zhang,[ab] Fenggang Liu,[ab] Dan Yang,[ab] Maolin Zhang,[ab] Shuhui Bo,[a] Xinhou Liu,[a] Ling Qiu[a] and Zhen Zhen*[a]

To improve poling efficiency of nonlinear optical (NLO) chromophore, we have designed and synthesized a chromophore containing two asymmetric donor-π-acceptor (D-π-A) chains. Two corresponding reference chromophores containing single D-π-A chain with malononitrile and tricyanofuran (TCF) as electron acceptors respectively, 8-hydroxy-1,1,7,7-tetramethyl-formyljulolidine as electron donor, have also been prepared to comparison. The macroscopic electro-optic activity of the three chromophores are investigated using guest-host doped polymer films (doping chromophores C1, C2 and C3 into amorphous polycarbonate (APC) with a loading density of 20 wt%). The poling efficiency (r_{33}/N) of united chromophore (10.71×10^{-20} pm g/(V molecules) at 1310 nm) is much higher than two reference chromophores (8.971×10^{-20}, 1.01×10^{-20} pm g/(V molecules) at 1310 nm), which is due to reduced intermolecular dipole-dipole interactions. Density Functional Theory (DFT) calculations indicate that the dipole moment (μ) of united chromophore (9.7D) decreases, comparing with the two reference chromophores (19.8D, 10.3D respectively). Furthermore, the united chromophore also exhibits excellent solubility in most common solvents, good transparency and high thermal stability (202 °C). These results show that this work might provide an available structure for boosting poling efficiency of NLO chromophore.

Introduction

With attractive application in photonic devices, organic electro-optic (EO) materials have continuously drawn great interest[1-4]. These new materials have many advantages: large EO coefficients, ultrafast response, high optical damage threshold, simple preparation and low cost[2, 5-7]. However, there are still some challenging topics, such as a trade-off between nonlinearity and transparency[8], efficient arrangement of NLO chromophores[9], which are needed to be solved in designing organic/polymeric second-order nonlinear optical materials.

In general, to achieve high EO efficiency, an organic material should be comprised of NLO chromophores with large first hyperpolarizability (β). A chromophore, which possesses a large first-hyperpolarizability, generally possesses a strong donor, a strong acceptor, and a long conjugated bridge[9]. This architecture inevitably means a large dipole moment. However, NLO chromophores with large values of β usually have large dipole moments, which will lead to an antiparallel pattern and reduce the macroscopic EO effect. An antiparallel pattern means unfavorable antiparallel packing of the chromophoric units. Macroscopic electro-optic effect, r_{33} results from microscopic molecular first hyperpolarizability(β). Antiparallel pattern means the efficiency of translating the molecular microscopic hyperpolarizability into themacroscopic EO activities is low[10]. Thus, it is essential to decrease the dipole moments and translate the large β values of the organic chromophores .

Up to now, two main solutions have been developed. One solution is molecular modification, such as employing special conjugated bridge[11-14], combining different kinds of conjugation bridge combinations[15-17]; the other solution is using different novel structures, such as Y-shaped[18, 19], H-shaped[20], star-shaped[21, 22] and Λ-shaped[23, 24], etc. These two main solutions are directly dependent on the degree of chromophore ordering obtained during poling. However, poling is a low-yield process[25], which is mainly due to the very strong interchromophore dipole–dipole interactions, leading to unfavorable antiparallel packing of the chromophoric units[9]. It has been found that site isolation of the chromophores, which could minimize the dipole–dipole interactions and improve the poling efficiency significantly[25]. The introduction of bulky substitutes into chromophore backbone is an effective way to site-isolate chromophores and reduce the dipole-dipole interactions[10]. Meanwhile, when chromophores are gathered in close proximity by covalent linking, self-orientation (driven by dipolar repulsion) and mutual polarisation effects will weak the intermolecular interactions and modulate their ground-state polarity. In this aspect, some innovative work has been done[26-28].

In this paper, we develop a second-order nonlinear chromophore with two asymmetric non-conjugated D-*π*-A units, then one of the D-*π*-A chains could be an isolation group for the another. Due to self-orientation and mutual polarisation effects , which might lead to antiparallel packing of two D-*π*-A units. It means the dipole moment of two D-*π*-A chains of united chromophore are opposite, decreasing the united chromophore's dipole moment dramatically. In this regard, we utilize 8-hydroxy-1,1,7,7-tetramethyl-formyljulolidine as electron donor and tricyanofuran (TCF) as electron acceptor for one D-*π*-A unit, while the other D-*π*-A unit has electron acceptor of malononitrile (Chart 1). Compared with other typical chromophores with two D-*π*-A chains, such as H-shaped chromophores[20], the significant difference is that our synthesized chromophore has two different D-*π*-A chains. Besides, the link of two D-*π*-A chains is flexible alkyl chain, while the link of typical H-shaped chromophores is fixed spacers[29, 30]. As far as we know, few related work has been reported in this novel structure.[26] The photophysical properties, thermal stability and nonlinear optical properties of the three chromophores are systematically studied. Compared with the reference chromophores C1 and C2 , chromophore C3 shows an enhanced poling efficiency (r_{33}/N) and decreasing dipole moment (μ). Furthermore, the united chromophore C3 shows excellent solubility in a series of solvents, good transparency and high thermal thermal stability (202 °C). Our results suggest that the structure of containing two different chromophores through flexible alkyl chain might be a useful approach for improving poling efficiency of NLO chromophore.

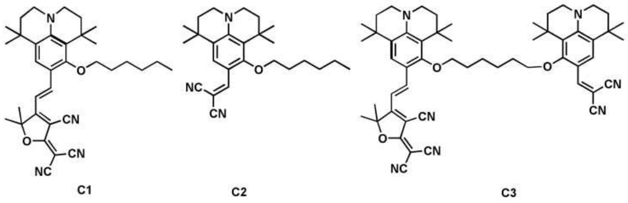

Chart 1. Structure of chromophores C1-C3

Results and Discussion

Synthesis of chromophores

Synthesis of C1, C2 and C3 chromophores are synthesized following the general route laid out in scheme 1. The 2-dicyanomethylene-3-cyano-4-methyl-2,5- dihydrofuran (TCF) is prepared according to the literature[31]. Compound 2 is prepared by a S_N2 substitution reaction of commercially available compound 1 with bromoethane. The same reaction is used for compound 3,which is obtained by substituting of compound 1 with 1,6-dibromohexane. Chromophore C1 is synthesized by Knoevenagel condensation of compound 2 and the TCF in 75% yield. Chromophores C2 is also synthesized by the same condensation of compound 2 and the malononitrile in 81% yield. Chromophores C3 are obtained by two steps of Knoevenagel condensation in 46% yield. All three chromophores are purified by column chromatography.

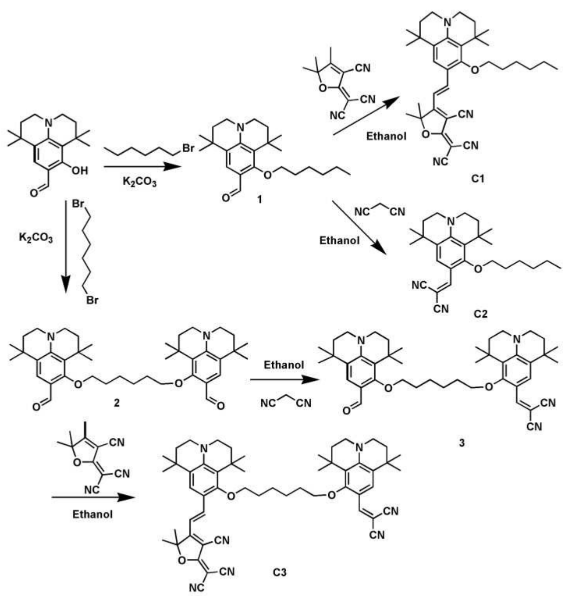

Scheme 1. Synthetic route of chromophores C1-C3

In order to understand the ground-state polarization of the three chromophores, the theoretically calculated parameters of chromophores C1, C2 and C3, including HOMO–LUMO energy gaps, the dipole moment (μ) and zero-frequency molecular first hyperpolarizability (β), are displayed in Table 1 and Table2. Fig.1 represents the electron density distribution of the HOMO and LUMO structures of chromophores C1, C2 and C3. The geometry optimization of three chromophores are shown in Fig.2. The DFT calculations are carried out at the hybrid B3LYP level by employing the split valence 6-31 g (d, p) basis set[32-34]**.** When we use theoretical calculation carefully, the method of DFT can be shown to give accurate descriptions of first-order hyperpolarizability for a number of chromophores. It is reinforced by theoretical calculations and optical characterizations that the β value has a close relationship with the substituents, steric hindrance, and intramolecular charge-transfer[35]**.** The scalar quantity of β can be computed from the x, y, and z components according following equation.

$$\beta=\sqrt{\beta_x{}^2+\beta_y{}^2+\beta_z{}^2}$$

$$\beta_i=\beta_{iii}+\frac{1}{3}\sum_{i\neq j}(\beta_{ijj}+\beta_{jij}+\beta_{jji}),i,\,j\in(x,y,z)$$

Due to the stronger electron-acceptor ability, chromophore C1 shows a larger β value (124× 10^{-30} esu) than that of chromophore C2 (24× 10^{-30} esu). Chromophore C3 (united D-π-A chains) exhibits a smaller β value (97× 10^{-30} esu) than chromophore C1, which is due to the antiparallel packing of two D-π-A chains, as are shown in Fig. 2. Interestingly, the sum of β value of chromophore C2 and C3 is nearly equal with the β value of chromophore C1. The results mean the D-π-A structure of each chain does not get damaged.

The frontier molecular orbitals are also used to characterize the chemical reactivity and kinetic stability of a molecule and to obtain qualitative information about the optical and electrical properties of molecules[36]. From the optimized structure of chromophore C1, C2 and C3, it is clearly noticed that the electron density is concentrated on the donor moiety at the HOMO state. For LUMO state, the electron density is concentrated on the acceptor moiety. Besides, the HOMO-LUMO energy gap is also used to understand the charge transfer interaction occurring in a chromophore molecule[37]. As showed in data, the HOMO energy of chromophore C3 is 0.022 eV lower than C1 (-5.642 eV vs. -0.562 eV), and the LUMO energy of chromophore C3 is 0.035 eV lower than that of C1 (-3.049 eV vs. -3.014 eV), which indicate the introduction of chromophore C2 influences the LUMO energy to a greater extent than the HOMO energy. Then, for chromophore C2, the HOMO energy is 0.001 ev higher than chromophore C3 (-0.5642 eV vs. -0.5643 eV), and the LUMO energy of chromophore C3 is 0.695 eV lower than that of C2 (-3.049 eV vs. -2.344 eV). These figures also mean the introduction of chromophore C1 has a greater on LUMO energy than HOMO energy. From Table 2, chromophore C3 has the lower energy gap ($\Delta E_{/(\mathrm{eV})}$ =2.593) than that of chromophore C1 and C2 ($\Delta E_{/(\mathrm{eV})}$ =3.299, $\Delta E_{/(\mathrm{eV})}$ =2.606) , which indicates that chromophore C3 has easier charge transfer ability[38].

Table 1 HOMO and LUMO energy levels, HOMO-LUMO energy gaps, and hyperpolarizability data using DFT calculations for chromophores C1, C2, C3

Chromophore	E_{HOMO}/(eV)[a]	E_{LUMO}/(eV)[b]	$\Delta E_{/(\mathrm{eV})}$[c]	$\beta_{/(10^{-30}\,\mathrm{esu})}$[d]
C1	-5.620	-3.014	2.606	124
C2	-5.643	-2.344	3.299	24
C3	-5.642	-3,049	2.593	97

The values of [a] E_{HOMO}, [b] E_{LUMO} and [d] β are calculated using Gaussian 03 at B3LYP/6-31g (d, p) level [c] ΔE = [b] E_{LUMO} - [a] E_{HOMO}

Table 2 Dipole moment of chromophores C1, C2 and C3.

Chromophore	μ_{TOT} (D)[a]	μ_X (D)	μ_Y (D)	μ_Z (D)
C1	19.8	19.0	5.6	0.8
C2	10.3	4.7	9.2	0.3
C3	9.7	4.0	8.9	0.5

[a] $\mu_{TOT}=\sqrt{\mu_X{}^2+\mu_Y{}^2+\mu_Z{}^2}$

The critical figure-of-merit, dipole moment (μ), demonstrates the effect of intermolecular interactions. Compared with C1, due to the self-orientation (driven by dipolar repulsion) of two reference chains, the μ_{TOT} of C3 decreases dramatically from 19.8 D to 9.7 D. Meanwhile, the μ_{TOT} of C3 also decreases from 10.3 D to 9.7 D compared with C2. Consequently, the modification successfully decreases the dipole moment of chromophore C3, the strength of dipole-dipole interaction might weaken due to the decreasing dipole moment, which is just as what we expect. DFT calculations mean liking two different D-π-A chains together, dipolar repulsions of two chains will decrease the dipole moment significantly. So, the work by us, might give a useful way to weaken the dipole-dipole interactions of chromophores.

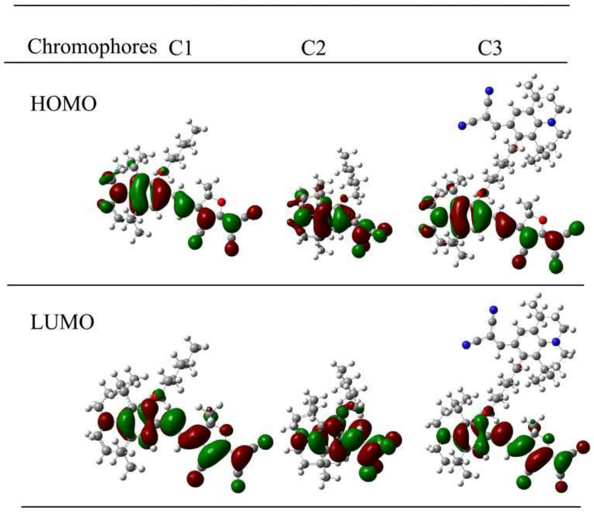

Fig. 1 The frontier molecular orbitals of chromophores C1,C2 and C3

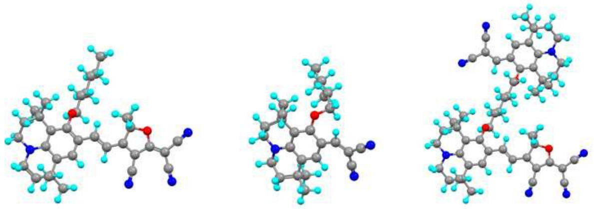

Fig. 2 The optimized structure of chromophore C1, C2 and C3

For studying the solvatochromic behavior of chromophores C1, C2 and C3, UV-Vis absorption spectra of three chromophores (c=1×10^{-5} mol/L) measured in a series of aprotic solvents with different polarity are displayed in Fig.3 and the spectra data is summarized in Table.3. From the Fig.3, it is obvious that the absorption maximum (λ_{max}) is significantly dependent on the solvent polarity. It could be found that three chromophores exhibit a distinct red-shift of the maximum absorption when gradually increasing solvent dielectric constants from 1, 4-dioxane to DMF. For chromophore C1, C2 and C3, the data of red-shift is 31nm, 12nm, 26nm, from 1, 4-dioxane to chloroform. From 1, 4-dioxane to DMF, for chromophore C1, C2 and C3 , the data of red-shift is 44nm, 18nm, 38nm, respectively. These results properly mean chromophores C1,C2 and C3 possess neutral ground state (in 1,4-dioxane and toluene) and then approach the cyanine limit (in DMF and Acetonitrile)[39].The full width at half maximum (FWHM) values of chromophore C2 lies in the range of 42 to 49 nm, which is smaller than chromophore C1 (from 65 to 94 nm). For chromophore C3, the FWHM values are from 67nm to 98 nm.Compared with chromophore C1 and C2, the larger FWHM of chromophore C3 suggest it can be polarized more efficiently.

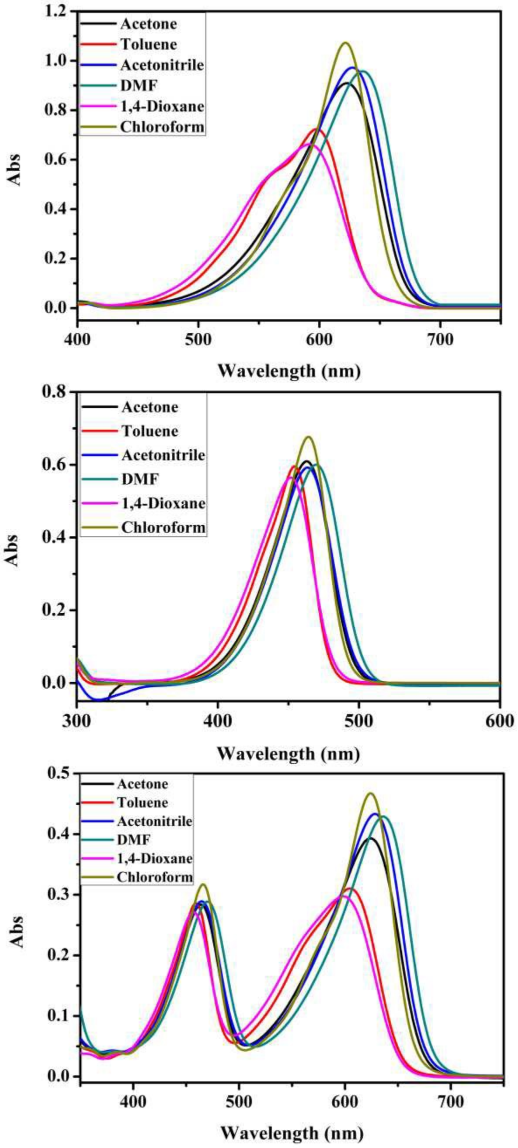

Fig. 3. UV-vis absorption spectra in six solvents (10^{-5} M) of varying dielectric constants at room temperature for chromophores C1-C3

Compared with chromophore C1 having a λ_{max} of 592 nm in 1, 4-dioxane, the λ_{max} of chromophore C3 with a red-shift by 6 nm. The same slight red-shift is also found in other solvents, such as 7nm in toluene and 2nm in acetonitrile for chromophore C3. The slight red-shift might be due to mutual polarisation effects of two D-π-A chains. These facts reflect the similar trend of a lower energy gap for chromophore C3 ,which is also in agreement with the theoretical calculations discussed above. Obviously, chromophore C3 has two absorption bands. The maximum absorption wavelength of two absorption bands of chromophore C3 shows no much difference with chromophores C1 and C2 in a series of solvents. It shows when linking two reference chains together through flexible alkyl chain, the change of charge-transfer energy in each D-π-A is independent. It means the D-π-A structure of each chain does not get damaged. Apart from that, the absorption band shapes of each D-π-A chain do not change at all, which also indicates the two D-π-A structures of chromophore C3 are intact. The UV-Vis data proves this linking two D-π-A chains by flexible alkyl chain, maintaining electronic transmission on two chains independent and integrity of each D-π-A chain.

For NLO chromophores, it is necessary to be thermally stable enough to withstand encountered high temperatures (>100 °C) in electric field poling and processing of chromophore/polymer materials. The thermal stability of three chromophores is investigated using thermogravimetric analysis (TGA) as shown in Fig. 5. Chromophores C1 and C2 exhibit good thermal stabilities with the thermal decomposition temperature (T_d) at a point at 176 °C and 226 °C respectively. The lower thermal stability of chromophore C1 can be attributed to the reduced stability of the TCF acceptor moiety.The novel chromophore C3 shows the decomposition temperature with a point of 202 °C, a slight increase with respect to chromophore C1, which means linking two different D-π-A chains together does not reduce thermo-stability of chromophore.

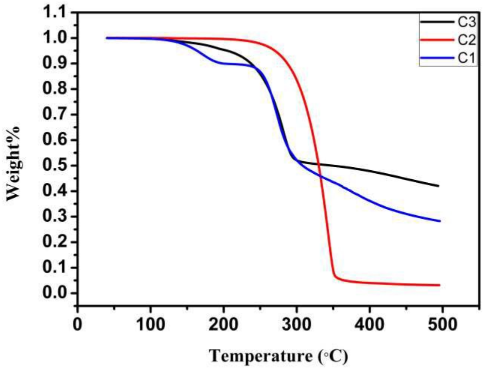

Fig. 5. Thermogravimetric analyses of the chromophores C1- C3

For studying EO property and poling efficiency of the three chromophores, guest-host polymers are generated by formulating three chromophores into amorphous polycarbonate (APC) using dibromomethane (CH_2Br_2) as solvent. The resulting solutions are filtered through a 0.2-μm PTFE filter and spin-coated onto indium tin oxide (ITO) glass substrates. Films of doped polymers are baked in a vacuum oven at 85°C overnight to ensure the removal of the residual solvent. The corona poling process is carried out at a temperature of 10 °C above the glass transition temperature (T_g) of the polymer. The r_{33} values are measured using the Teng-Man simple reflection technique at the wavelength of 1310 nm using a carefully selected thin ITO electrode with low reflectivity and good transparency in order to minimize the contribution from multiple reflections.[40]

The r_{33} values are related to the chromophore number density (N), β, and poling efficiency, described by the $\langle\cos 3\theta\rangle$ order parameter, as indicated by[41]:

$$r_{33} = \left|2Nf(\omega)\beta\left\langle\cos^3\theta\right\rangle / n^4\right|$$

where N represents the aligned chromophore number density (molecules per cm^3) in the polymer host, n is the refractive index , and f (ω) is the product of local-field (Debye–Onsager) factors. n and f (ω) remain relatively constant for related chromophores at similar loading densities. cos^3(θ) is the acentric order parameter. θ is the angle between the permanent dipole moment of chromophores and the applied electric-field. To have meaningful analysis, the loading densities of the chromophores are presented in terms of N, ensuring normalization of observed r_{33} values for the chromophore content[25]. The r_{33} values of films containing chromophore C1 (film-A), C2 (film-B) and C3 (film-C) are measured in the same loading densities (20 wt%), as shown in Table 3.

Film-A are prepared with 20 total chromophore wt %, and the corresponding N is 2.23 × 10^{20} molecules/g. Film-A are poled between 114 °C and 139 °C with an electric field of 10000-13000V for 10 min. The optimized conditions are determined to be 134 °C under an electric field of 12000V, with resulting r_{33} value of 20 pm/V. Dividing the observed r_{33} by *N* yields a value of 8.97 × 10^{-19} p mg/(V molecules), which effectively normalizes the r_{33} value for the relative chromophore content. This figure indicates the effective poling efficiency of this chromophore.

Film-B are also prepared with 20 total chromophore wt %, corresponding to 2.97 × 10^{20} molecules/g, and poled between 110°C and 130°C with an electric field of 10000-12000V for 10 min. The optimized conditions are determined to be 120°C under an electric field of 11000 V, and the resulting r_{33} value is 3 pm/V. Dividing the observed r_{33} by *N* yields a value of 1.01 × 10^{-19} pm g/(V molecules). Comparing this value with that of chromophore C1 suggests chromophore C2 has a significantly reduced poling efficiency, probably due to the much smaller value of β than that of chromophore C1 .

Film-C are prepared with 20 total chromophore wt % , corresponding to 1.40 × 10^{20} molecules/g. Due to the introduction of rigid group in chromophore C3, higher voltage of 12500V is applied. At 20 wt % , the poling conditions are optimized with 12500V at 139 °C .The maximum r_{33} value of 15 pm/V for Film-C is achieved after 10 minutes' poling. When prolonging the poling time, r_{33} value decreases. Normalizing this with N yields a value of 10.71 pm g/(V molecules) . Thus, while the absolute r_{33} of Film-C is smaller than that of Film-A, the effective poling efficiency appears to be higher. Meanwhile, the absolute r_{33} of Film-C is higher than that of Film-B, the effective poling efficiency seems higher as well. For Film-C and Film-A ,one possible explanation for the observed increase in poling efficiency arises from the reducing dipole moment, because of the antiparallel packing of two D-*π*-A units. It means when the value of β is nearly equal, dipole moment is critical in poling efficiency. For Film-C and Film-B, one possible explanation for the observed increase in poling efficiency arises from the high value of β. It means when the value of dipole moment is nearly equal, β plays a key role in poling efficiency. Moreover, it is helpful to determine the relative contributions of β and dipole moment to the poling efficiency obtained for Film-A, Film-B and Film-C. Besides, as the structure is designed to minimize intermolecular dipole–dipole interactions, it is possible that the reducing dipole moment is beneficial to decrease intermolecular dipole–dipole interactions .It means novel structure also provides effective site isolation to decrease the strong electrostatic interactions among chromophores, which suggests that the structure might be desirable in reducing dipole–dipole interactions and prevailing parallel pattern.

Table 3 r_{33} values (20 wt% doping content) and relative poling efficiencies of chromophore C1,C2,C3.

Chromophore	C1	C2	C3
r_{33}/(pm/v)[a]	20	3	15
N[b]	2.23	2.97	1.40
r_{33}/N[c]	8.97	1.01	10.71
Tg(□)[d]	124	110	129

[a] Experimental value from simple reflection at 1310 nm. [b] Chromophore number density; in units of ×10^{20} molecules/g. [c] r_{33} normalized by chromophore number density; in units of ×10^{-20} pm g/(V molecules). [d] Glass transition temperature (Tg) is measured by DSC, with a heating rate of 10□/min in nitrogen.

Conclusion

In summary, a novel structure of nonlinear optical chromophore, containing two asymmetric donor-*π*-acceptor (D-*π*-A) chains has been synthesized and characterized. Two corresponding reference chromophores have also been prepared for comparison. Theoretical and experimental investigations suggest that this structure is useful for improving poling efficiency. Linking two D-*π*-A chains together with flexible alkyl chain leads to antiparallel packing of two D-*π*-A units, which is due to self-orientation and mutual polarisation effects. It means the dipole moments of two D-*π*-A chains of novel chromophore are opposite, which decreases the novel chromophore's dipole moment dramatically. DFT calculations show that the dipole moment of C3 chromophore is close to the difference of the two component chromophores. From linear properties of chromophores C1, C2 and C3 determined in different polarity solvents, meaning chromophore C3 can be polarized more easily, which is consistent with DFT calculations. Apart from that, chromophore C3 is thermally stable enough to withstand encountered high temperatures with thermal stability (202°C).What is more important , the poling efficiency (r_{33}/N) of novel chromophore C3 (10.71×10^{-20} pm g/(V molecules) at 1310 nm) is much higher than two reference chromophores. This work demonstrates the new structure of NLO chromophore is a promising way to boost poling efficiency and may be suitable for EO materials and devices application.

Experimental section

Materials and instruments

All solvents and chemicals are commercially available and used without further purification unless otherwise stated. N, N-dimethyl formamide (DMF) is distilled over calcium hydride and stored over molecular sieves (pore size 3Å). Thin layer chromatography (TLC) analyses are carried out on 0.25mm thick precoated silica plates and spots are visualized under UV light. Chromatography on silica gel is carried out on Kieselgel (200-300 mesh).

The UV-Vis experiments are performed on Cary 5000 photo spectrometer. The TGA is determined by TA5000-2950TGA (TA co) with a heating rate of 10 °C min^{-1} under the protection of nitrogen. ^{1}HNMR and ^{13}C NMR spectra are determined using an Advance Bruker 400M (400 MHz) NMR spectrometer (tetramethylsilane as internalreference). The MS spectra is obtained on MALDI-TOF (Matrix Assisted Laser Desorption/Ionization of Flight) on BIFLEXIII (Broker Inc.) spectrometer.

Synthesis

Synthesis of compound 2

To a stirred solution of compound 1 (2.72 g, 10 mmol) and 1-bromohexane (2.16 g, 13 mmol) in DMF (30 mL) anhydrous potassium carbonate (1.79 g, 13 mmol) are added. The reaction mixture is heated at 120 °C under nitrogen for 24 h and then poured into water. The organic phase is extracted by ethyl acetate (AcOEt), and dried over $MgSO_4$. After removal of the solvent under reduced pressure, the crude product is purified by silica chromatography, eluting with (AcOEt: petroleum ether= 1:40, v/v) to give compound 1 (2.96 g, yield: 83%). ^{1}H NMR (400 MHz, $CDCl_3$, δ ppm): δ 9.96 (s, 1H), 7.59 (s, 1H), 3.96 (t, J = 6.9 Hz, 2H), 3.29 (t, 2H), 3.23 (t, 2H), 1.87 (m, 2H), 1.71 (m, 4H), 1.46 (dd, J = 8.6, 4.1 Hz, 2H), 1.43 (s, 6H), 1.35 (m, 4H), 1.26 (s, 6H), 0.91 (t, J = 7.0 Hz, 3H). ^{13}C NMR (100 MHz, $CDCl_3$, δ ppm) δ 187.75, 162.12, 148.20, 126.06, 125.29, 120.71, 117.26, 78.88, 47.46, 46.82, 39.41, 35.70, 32.44, 32.04, 31.74, 30.25, 30.01, 29.73, 25.63, 22.56, 14.01. MALDI-TOF-MS (m/z): calcd for $C_{23}H_{35}NO_2$: 358.0 ; found: 359.2.

Synthesis of compound 3

To a stirred solution of compound 1 (2.72 g, 10 mmol) and 1,6-Dibromohexane (1.22 g, 5 mmol) in DMF (30 mL) anhydrous potassium carbonate (1.79 g, 13 mmol) are added. The reaction mixture is heated at 120 °C under nitrogen for 24 h and then poured into water. The organic phase is extracted by ethyl acetate (AcOEt), and dried over $MgSO_4$. After removal of the solvent under reduced pressure, the crude product is purified by silica chromatography, eluting with (AcOEt: petroleum ether = 1:7, v/v) to give compound 3 (1.95 g, yield: 63%). ^{1}H NMR (400 MHz, $CDCl_3$, δ ppm): δ 9.87 (s, 2H), 7.50 (s, 2H), 3.90 (t, *J* = 6.8 Hz ,4H), 3.23 (dd, *J* = 14.0, 8.0 Hz, 4H), 3.18 – 3.12 (m, 4H), 1.87 (dd, *J* = 21.4, 15.0 Hz, 4H) , 1.63 (td, *J* = 10.2, 6.0 Hz, 8H),1.50 (s, 4H),1.36 (s,12H),1.18 (s, 12H).^{13}C NMR (100 MHz, $CDCl_3$, δ ppm) δ 187.81, 162.06, 148.24, 126.12, 125.49, 120.78, 117.29, 78.68, 47.51, 46.87, 39.43, 35.74, 32.50, 32.01, 30.27, 30.03, 29.79, 26.09. MALDI-TOF-MS (m/z): calcd for $C_{40}H_{56}N_2O_4$: 628.9 ; found: 629.3.

Synthesis of chromophore C1

To a solution of compound 2 0.534g (1.50 mmol) and the TCF acceptor (0.36 g, 1.8 mmol) in EtOH (30 mL), several drops of triethylamine are added. The reaction is allowed to stir at 90 °C for 2 h and then cooled to room temperature. After removal of the solvent under reduced pressure, the crude product is purified by silica chromatography, eluting with (AcOEt: petroleum ether = 1:5, v/v) to give compound C1 (0.61 g, yield: 75%). ^{1}H NMR (400 MHz, $CDCl_3$, δ ppm) δ 7.73 (d, J = 15.6 Hz, 1H), 7.42 (s, 1H), 6.73 (d, J = 15.8 Hz, 1H), 3.79 (t, J = 7.3 Hz, 2H), 3.42 (t, J = 6.2 Hz, 2H), 3.35 (t, 2H), 1.92 (m, 2H), 1.76 (s, 6H), 1.75 – 1.72 (m, 2H), 1.43 (s, 6H), 1.34 (dd, J = 7.3, 3.4 Hz, 4H), 1.30 (s, 6H), 0.91 (t, 3H). ^{13}C NMR (100 MHz, $CDCl_3$, δ ppm) δ 174.07, 160.68, 149.17, 143.87, 130.91, 128.85, 128.32, 124.39, 122.44, 115.50, 113.35, 112.54, 111.90, 107.18, 96.06, 71.79, 65.55, 47.94, 47.28, 38.88, 35.12, 32.50, 32.09, 31.75, 29.72, 29.31, 27.12, 25.62, 22.57, 13.99. MALDI-TOF-MS (m/z):calcd for $C_{34}H_{42}N_4O_2$: 538.3; found: 539.1.

Synthesis of chromophore C2

To a solution of compound 2 0.715g (2.0 mmol) and the Malononitrile acceptor (0.198 g, 3.0 mmol) in EtOH (30 mL), several drops of triethylamine are added. The reaction is allowed to stir at 90 °C for 2 h and then cooled to room temperature. After removal of the solvent under reduced pressure, the crude product is purified by silica chromatography, eluting with (AcOEt: petroleum ether = 1:7, v/v) to give compound C2 (0.65 g, yield: 81%). ^{1}H NMR (400 MHz, $CDCl_3$, ppm):8.17 (s, 1H), 7.70 (s, 1H), 3.79 (t, *J* = 6.8 Hz, 2H), 3.39 (t, *J* = 6.2 Hz, 2H), 3.35 – 3.28 (m, 2H), 1.93 – 1.82 (m, 2H), 1.76 – 1.68 (m, 4H), 1.49 (dd, *J*=14.6, 7.1Hz, 2H), 1.40 (s, 6H), 1.39-1.34 (m, 4H), 1.29 (s, 6H), 0.93 (t, *J*=6.8Hz, 3H) ^{13}C NMR(100MHz,$CDCl_3$,δ ppm) δ 160.30,152.68,149.35,127.33, 125.14,121.62,115.97,112.85,78.62,47.91,47.14,38.97,35.28,32.46,31.71,30.03,29.75,29.43,25.68,22.58,13.98. MALDI-TOF-MS (m/z): calcd for $C_{26}H_{35}N_3O$: 405.6; found: 406.4.

Synthesis of compound 4

To a solution of compound 3 0.626g (1.0 mmol) and the Malononitrile acceptor (0.079 g, 1.2 mmol) in EtOH (30 mL), several drops of triethylamine are added. The reaction is allowed to stir at 90 °C for 2 h and then cooled to room temperature. After removal of the solvent under reduced pressure, the crude product is purified by silica chromatography, eluting with (AcOEt: petroleum ether= 1:7, v/v) to give compound 4 (0.49 g, yield: 72%).^{1}H NMR (400 MHz, $CDCl_3$, δ ppm): δ 9.94 (s, 1H), 8.17 (s, 1H), 7.70 (s, 1H), 7.58 (s, 1H), 3.99 (t, *J* = 6.6 Hz, 2H), 3.81 (t, *J* = 6.6 Hz, 2H), 3.39 (t, *J* = 6.0 Hz, 2H), 3.31 (dd, *J* = 12.4, 7.2 Hz, 4H), 3.23 (t, 2H), 1.93 (d, *J* = 6.0 Hz, 4H), 1.71 (t, *J* = 9.9 Hz ,8H), 1.60 (s, 4H),1.44 (s, 6H), 1.40 (s, 6H), 1.29 (s, 6H), 1.27 (s, 6H). ^{13}C NMR (100MHz,$CDCl_3$, δppm) δ 187.77,162.02,160.16,152.46,149.36,148.27,127.25,126.13, 125.55,125.03,121.50,120.81,117.24,117.14,116.00,112.66,78.55,78.40,68.40,47.87,47.51,47.06,46.87,39.41,38.79,35.72,35.08,32.50,32.41,32.36,32.08,30.26,29.99,29.80,29.66,29.38, 26.05.MALDI-TOF-MS (m/z): calcd for $C_{43}H_{56}N_4O_3$: 676.9 ; found: 678.3

Synthesis of chromophore C3

To a solution of compound 4 0.677g (1.0 mmol) and the TCF acceptor (0.238 g, 1.2 mmol) in EtOH (30 mL), several drops of triethylamine are added. The reaction is allowed to stir at 90 °C for 2 h and then cooled to room temperature. After removal of the solvent under reduced pressure, the crude product is purified by silica chromatography, eluting with (AcOEt: petroleum ether = 1:3, v/v) to give compound C3 (0.54g, yield: 63%). ^{1}H NMR (400 MHz, $CDCl_3$, δ ppm): δ 8.17 (s, 1H), 7.82 (d, J = 15.7 Hz,1H), 7.68 (s, 1H), 7.41 (s, 1H), 6.68 (d, J = 15.6 Hz, 1H), 3.89 – 3.77 (m, 4H), 3.45 – 3.38 (m, 4H), 3.34 (d, J = 4.6 Hz, 4H), 2.17 (s, 6H), 2.00 (s, 2H), 1.90 (d, J = 6.7 Hz, 2H), 1.75 (s, 8H), 1.64 (s, 2H), 1.58 (s, 2H), 1.44 (s, 6H), 1.40 (s, 6H),1.31 (s, 6H), 1.26 (s, 6H). ^{13}C NMR (100 MHz, $CDCl_3$, δ ppm) δ 188.41, 177.35,174.00, 160.72, 160.13, 152.47, 149.35,148.27, 130.93, 128.85, 128.31,127.31, 125.04 , 122.54, 121.47, 117.26, 115.98, 115.54, 113.42, 112.57, 107.04 , 96.11, 78.24, 68.16, 62.79, 47.90, 47.30, 47.07,38.78, 38.74,35.10, 32.59, 32.42,32.39, 32.09, 30.08, 30.02,29.72, 29.64, 29.41,29.38, 27.06, 26.04, 25.68, 19.17.MALDI-TOF-MS (m/z): calcd for $C_{54}H_{63}N_7O_3$: 858.1 ; found: 859.3

Acknowledgments

We are grateful to the Directional Program of the Chinese Academy of Sciences (KJCX2.YW.H02), Innovation Fund of Chinese Academy of Sciences (CXJJ-11-M035) and National Natural Science Foundation of China (No. 11104284 and No. 61101054) for the financial support.

Notes and references

[a] *Key Laboratory of Photochemical Conversion and Optoelectronic Materials, Technical Institute of Physics and Chemistry, Chinese Academy of Sciences, Beijing 100190, P. R..China. E-mail: zhenzhenipc@gmail.com;*

[b] *University of Chinese Academy of Sciences, Beijing 100049, China*

†Electronic supplementary information (ESI) available: Quantum mechanical calculations,TGA curves, ^{1}H and ^{13}C NMR spectra of compounds.

1. P. A. Sullivan and L. R. Dalton, *Acc. Chem. Res.*, 2010, 43, 10-18.
2. F. Liu, H. Wang, Y. Yang, H. Xu, M. Zhang, A. Zhang, S. Bo, Z. Zhen, X. Liu and L. Qiu, *J. Mater. Chem. C*, 2014, 2, 7785-7795.
3. L. R. Dalton, P. A. Sullivan and D. H. Bale, *Chem. Rev.*, 2010, 110, 25-55.
4. B. J. Coe, S. P. Foxon, E. C. Harper, M. Helliwell, J. Raftery, C. A. Swanson, B. S. Brunschwig, K. Clays, E. Franz, J. Garin, J. Orduna, P. N. Horton and M. B. Hursthouse, *J. Am. Chem. Soc.*, 2010, 132, 1706-1723.
5. Y. V. Pereverzev, K. N. Gunnerson, O. V. Prezhdo, P. A. Sullivan, Y. Liao, B. C. Olbricht, A. J. P. Akelaitis, A. K. Y. Jen and L. R. Dalton, *J. Phys. Chem. C*, 2008, 112, 4355-4363.
6. K. H. Park, J. T. Lim, S. Song, Y. S. Lee, C. J. Lee and N. Kim, *Reactive & Functional Polymers*, 1999, 40, 177-184.
7. A. Zhang, H. Xiao, S. Cong, M. Zhang, H. Zhang, S. Bo, Q. Wang, Z. Zhen and X. Liu, *J. Mater. Chem. C*, 2014.
8. T. Verbiest, S. Houbrechts, M. Kauranen, K. Clays and A. Persoons, *J. Mater. Chem.*, 1997, 7, 2175-2189.
9. M. J. Truitt, S. S. Toporek, R. Rovira-Truitt and J. L. White, *J. Am. Chem. Soc.*, 2006, 128, 1847-1852.
10. J. Wu, C. Peng, H. Xiao, S. Bo, L. Qiu, Z. Zhen and X. Liu, *Dyes and Pigments*, 2014, 104, 15-23.
11. J. A. Hansen, J. Becher, J. O. Jeppesen, E. Levillain, M. B. Nielsen, B. M. Petersen, J. C. Petersen and Y. Sahin, *J. Mater. Chem.*, 2004, 14, 179-184.
12. G. Hennrich, M. T. Murillo, P. Prados, K. Song, I. Asselberghs, K. Clays, A. Persoons, J. Benet-Buchholz and J. de Mendoza, *Chem. Commun.*, 2005, 2747-2749.
13. F. Vocanson, P. Seigle-Ferrand, R. Lamartine, A. Fort, A. W. Coleman, P. Shahgaldian, J. Mugnier and A. Zerroukhi, *J. Mater. Chem.*, 2003, 13, 1596-1602.
14. C. F. Shu, Y. C. Shu, Z. H. Gong, S. M. Peng, G. H. Lee and A. K. Y. Jen, *Chem. Mater.*, 1998, 10, 3284-3286.
15. T. Nanba, A. Obuchi, H. Izumi, Y. Sugiura, J. Y. Xu, J. Uchisawa and S. Kushiyama, *Chem. Commun.*, 2001, 173-174.
16. D. R. Kanis, M. A. Ratner, T. J. Marks and M. C. Zerner, *Chem. Mater.*, 1991, 3, 19-22.
17. J. Abe, Y. Shirai, N. Nemoto and Y. Nagase, *J. Phys. Chem. A*, 1997, 101, 1-4.
18. J. Ren, S.-M. Wang, L.-F. Wu, Z.-X. Xu and B.-H. Dong, *Dyes and Pigments*, 2008, 76, 310-314.
19. A. Carella, F. Borbone, U. Caruso, R. Centore, A. Roviello, A. Barsella and A. Quatela, *Macromol. Chem. Phys.*, 2007, 208, 1900-1907.
20. C.-Z. Zhang, C. Lu, J. Zhu, C.-Y. Wang, G.-Y. Lu, C.-S. Wang, D.-L. Wu, F. Liu and Y. Cui, *Chem. Mater.*, 2008, 20, 4628-4641.
21. S. Brasselet, F. Cherioux, P. Audebert and J. Zyss, *Chem. Mater.*, 1999, 11, 1915-1920.
22. T. M. Figueira-Duarte, J. Clifford, V. Amendola, A. Gegout, J. Olivier, F. Cardinal, M. Meneghetti, N. Armaroli and J. F. Nierengarten, *Chem. Commun.*, 2006, 2054-2056.
23. C. R. Moylan, S. Ermer, S. M. Lovejoy, I. H. McComb, D. S. Leung, R. Wortmann, P. Krdmer and R. J. Twieg, *J. Am. Chem. Soc.*, 1996, 118, 12950-12955.
24. W. J. Kuo, G. H. Hsiue and R. J. Jeng, *J. Mater. Chem.*, 2002, 12, 868-878.
25. S. R. Hammond, O. Clot, K. A. Firestone, D. H. Bale, D. Lao, M. Haller, G. D. Phelan, B. Carlson, A. K. Y. Jen, P. J. Reid and L. R. Dalton, *Chem. Mater.*, 2008, 20, 3425-3434.
26. V. Parthasarathy, R. Pandey, F. Terenziani, P. K. Das and M. Blanchard-Desce, *PCCP*, 2014, 16, 9096-9103.
27. H. J. Deussen, E. Hendrickx, C. Boutton, D. Krog, K. Clays, K. Bechgaard, A. Persoons and T. Bjornholm, *J. Am. Chem. Soc.*, 1996, 118, 6841-6852.
28. P. J. A. Kenis, O. F. J. Noordman, S. Houbrechts, G. J. van Hummel, S. Harkema, F. van Veggel, K. Clays, J. F. J. Engbersen, A. Persoons, N. F. van Hulst and D. N. Reinhoudt, *J. Am. Chem. Soc.*, 1998, 120, 7875-7883.
29. C.-Z. Zhang, C. Lu, J. Zhu, G.-Y. Lu, X. Wang, Z.-W. Shi, F. Liu and Y. Cui, *Chem. Mater.*, 2006, 18, 6091-6093.
30. Z. Liu, G.-Y. Lu and J. Ma, *J. Phys. Org. Chem.*, 2011, 24, 568-577.
31. M. Q. He, T. M. Leslie and J. A. Sinicropi, *Chem. Mater.*, 2002, 14, 2393-2400.
32. R. M. Dickson and A. D. Becke, *J. Chem. Phys.*, 1993, 99, 3898-3905.
33. M. Frisch, G. Trucks, H. Schlegel, G. Scuseria, M. Robb, J. Cheeseman, J. Montgomery Jr, T. Vreven, K. Kudin and J. Burant, *Gaussian Inc., Pittsburgh, PA*, 2003.
34. P. Fuentealba, *Physical Review A*, 1992, 45, 6891-6894.
35. K. S. Thanthiriwatte and K. M. N. de Silva, *Journal of Molecular Structure-Theochem*, 2002, 617, 169-175.
36. R. Ma, P. Guo, L. Yang, L. Guo, X. Zhang, M. K. Nazeeruddin and M. Graetzel, *J. Phys. Chem. A*, 2010, 114, 1973-1979.
37. J. Wu, J. Liu, T. Zhou, S. Bo, L. Qiu, Z. Zhen and X. Liu, *Rsc Advances*, 2012, 2, 1416-1423.
38. R. V. Solomon, P. Veerapandian, S. A. Vedha and P. Venuvanalingam, *J. Phys. Chem. A*, 2012, 116, 4667-4677.

39. P.-A. Bouit, C. Aronica, L. Toupet, B. Le Guennic, C. Andraud and O. Maury, *J. Am. Chem. Soc.*, 2010, 132, 4328-4335.
40. C. C. Teng and H. T. Man, *Appl. Phys. Lett.*, 1990, 56, 1734-1736.
41.L. R. Dalton, P. A. Sullivan, D. H. Bale and B. C. Bricht, *Solid-State Electronics*, 2007, 51, 1263-1277.